AGU100 ADVANCING EARTH AND SPACE SCIENCE

Geophysical Research Letters

RESEARCH LETTER

10.1029/2018GL078731

Special Section:
Initial results of the ERG(Arase) project and multi-point observations in geospace

Key Points:
- Fast mode Pi2 waves and toroidal standing Alfven waves were simultaneously observed at different magnetic latitudes
- The toroidal waves last longer than the fast mode Pi2 waves
- Mass density is estimated from the frequency of the toroidal waves

Correspondence to:
K. Takahashi,
kazue.takahashi@jhuapl.edu

Citation:
Takahashi, K., Denton, R. E., Motoba, T., Matsuoka, A., Kasaba, Y., Kasahara, Y., et al. (2018). Impulsively excited nightside ultralow frequency waves simultaneously observed on and off the magnetic equator. *Geophysical Research Letters*, *45*, 7918–7926. https://doi.org/10.1029/2018GL078731

Received 11 MAY 2018
Accepted 14 JUL 2018
Accepted article online 24 JUL 2018
Published online 17 AUG 2018

Impulsively Excited Nightside Ultralow Frequency Waves Simultaneously Observed on and off the Magnetic Equator

Kazue Takahashi[1], Richard E. Denton[2], Tetsuo Motoba[1], Ayako Matsuoka[3], Yasumasa Kasaba[4], Yoshiya Kasahara[5], Mariko Teramoto[6], Masafumi Shoji[6], Naoko Takahashi[7], Yoshizumi Miyoshi[6], Masahito Nosé[8], Atsushi Kumamoto[4], Fuminori Tsuchiya[4], Robert J. Redmon[9], and Juan V. Rodriguez[9,10]

[1]The Johns Hopkins University Applied Physics Laboratory, Laurel, MD, USA, [2]Department of Physics and Astronomy, Dartmouth College, Hanover, NH, USA, [3]Institute of Space and Astronautical Science, Sagamihara, Japan, [4]Department of Geophysics, Tohoku University, Sendai, Japan, [5]Graduate School of Natural Science and Technology, Kanazawa University, Kanazawa, Japan, [6]Institute of Space-Earth Environmental Research, Nagoya University, Nagoya, Japan, [7]Graduate School of Science, Department of Earth and Planetary Science, The University of Tokyo, Tokyo, Japan, [8]Graduate School of Science, Kyoto University, Kyoto, Japan, [9]National Centers for Environmental Information, National Oceanic and Atmospheric Administration, Boulder, CO, USA, [10]Cooperative Institute for Research in Environmental Sciences, University of Colorado at Boulder, Boulder, CO, USA

Abstract The Arase spacecraft is capable of observing ultralow frequency waves in the inner magnetosphere at intermediate magnetic latitudes, a region sparsely covered by previous spacecraft missions. We report a series of impulsively excited fundamental toroidal mode standing Alfvén waves in the midnight sector observed by Arase outside the plasmasphere at magnetic latitudes 13–24°. The wave onsets are concurrent with Pi2 onsets detected by the Van Allen Probe B spacecraft at the magnetic equator in the duskside plasmasphere and by ground magnetometers at low latitudes. The duration of each toroidal wave packet is ~20 min, which is much longer than that of the corresponding Pi2 wave packet. The toroidal waves cannot be the source of high-latitude Pi2 waves because they were not detected on the ground near the magnetic field footprint of Arase. Overall, the toroidal wave event lasted more than 2 hr and allowed us to use the wave frequency to estimate the plasma mass density at $L = 6.1$–8.3. The mass density (in amu/cm^3) is higher than the electron density (cm^{-3}) by a factor of ~6, which implies that 17–33% of the ions were O^+.

Plain Language Summary Magnetospheric substorms begin with a sudden change of the configuration of the magnetotail, which excites magnetohydrodynamic waves with periods of the order of 100 s. The Arase satellite detects these waves at distances less than ~6 Earth radii and magnetic latitudes as high as ~40°, a region sparsely covered by previous spacecraft missions. On 24 May 2017, Arase, located off the equator, observed substorm-associated resonant oscillation of magnetic field lines (standing waves) continuously for 2 hr, whereas a Van Allen Probes spacecraft, located on the equator, observed short-lived oscillations with different frequencies. This multipoint observation indicates that different wave modes are excited from a common impulsive source located in the near-Earth magnetotail. The waves at Arase allow us for the first time to continuously monitor the plasma mass density in the nightside magnetosphere during substorms.

1. Introduction

Pi2 waves (or pulsations), with periods usually in the range 40–150 s, are detected whenever the magnetotail undergoes a rapid configurational change, typically at the beginning of a magnetospheric substorm. When observed near the magnetic equator, the waves exhibit properties of magnetohydrodynamic fast mode waves (Takahashi et al., 2003). While the origin of the periodicity of the fast mode waves is still a subject of ongoing research (e.g., Panov et al., 2014), the fast mode waves inevitably couple to shear Alfvén waves in the inhomogeneous magnetospheric plasma through the field line resonance process (Tamao, 1965), and the consequence of the coupling by itself is an important topic for scientific research. For instance, Alfvén waves propagate to the ionosphere along the background magnetic field and may contribute to formation of auroral arcs (Samson et al., 1996). Also, detection of the waves on the nightside enables modeling of the plasma mass density there using magnetoseismic techniques (Takahashi et al., 2004). Until now, observations of Pi2 waves and associated Alfvén waves have been made mostly using equatorial satellites such as Active Magnetospheric Particle Tracer Explorers Charge Composition Explorer (orbit inclination 5°; Takahashi et al., 1996) or polar-orbiting satellites such as Akebono (75°; Osaki et al., 1998), Dynamics Explorer-1 (90°; Teramoto et al., 2011), and Polar (79°; Keiling et al., 2003). With the launch of the Arase spacecraft, which has an intermediate orbital inclination of 31° and an apogee geocentric distance of 6.0 R_E, we now have the opportunity to simultaneously observe Pi2 waves and Alfvén waves by different spacecraft in the inner magnetosphere, including the relatively unexplored dipole magnetic latitudes (MLATs) of up to ±42°. This paper presents simultaneous observations of equatorial fast mode Pi2 waves by the Van Allen Probe B spacecraft and off-equatorial Alfvén waves by the Arase spacecraft (Miyoshi et al., 2018). Although these waves are simultaneously excited, the wave properties differ significantly between these spacecraft. We discuss possible reasons for this difference and also demonstrate that Alfvén waves observed by Arase provide us with a unique means to estimate the plasma mass density on the nightside.

2. Data

2.1. Wave Properties

The ultralow frequency waves selected for analysis occurred between 0100 and 0300 UT on 24 May 2017. Figure 1a shows L versus magnetic local time (MLT) coordinates of three satellites and three ground magnetometer stations during the 0030–0300 UT interval, where L is the geocentric distance to the point where the field line crosses the dipole equator. This L parameter is defined using the T89c model magnetic field (Tsyganenko, 1989), denoted $\mathbf{B}_{T89c}$, for Arase and Leirvogur (LRV) and a centered dipole for the other observatories. Geostationary Operational Environmental Satellite (GOES)-13 was in the premidnight sector, where substorm-associated magnetic field and particle flux variation is statistically prominent (e.g., Lopez et al., 1990). Van Allen Probe B was moving to lower L in the dusk sector, whereas Arase was moving to higher L in the postmidnight sector. Figure 1b shows that Van Allen Probe B was very close to the magnetic equator with MLAT between −1.8° and 2.5°, whereas Arase was off the equator at MLAT = 13–24°. The $\mathbf{B}_{T89c}$ field line passing Arase crosses the magnetic equator at the geocentric distance of 6.2 R_E at 0100 UT (red dashed line) and 8.2 R_E at 0300 UT (red solid line). Tailward stretching of these field lines is moderate, which implies that the cross-tail current within ∼8 R_E was weak during the wave events reported here.

Figure 1c shows the electron density at Van Allen Probe B (Kurth et al., 2015) and Arase (Kasahara et al., 2018; Kumamoto et al., 2018) on the relevant orbit legs as a function of dipole L. The thick green lines indicate the density values during the 0100–0300 UT interval. Arase encountered the plasmapause at L ∼ 5, and the spacecraft was clearly outside the plasmasphere during the selected 2-hr interval. In contrast, Van Allen Probe B remained in the plasmasphere.

Figures 1d–1l show time series plots of the auroral electrojet (AE) index; energetic proton fluxes at GOES-13 (Rodriguez, 2014); magnetospheric magnetic field at GOES-13 (Singer et al., 1996), Arase (Matsuoka et al., 2018), and Van Allen Probe B (Kletzing et al., 2013); and ground magnetic field at LRV, San Juan (SJG), and Honolulu (HON). The spacecraft magnetic field data are given in the locally defined right-handed orthogonal coordinates ν-ϕ-μ, where $\mathbf{e}_\nu$ (radially outward) and $\mathbf{e}_\phi$ (eastward) are perpendicular to $\mathbf{B}_{T89c}$ and $\mathbf{e}_\mu$ is parallel to $\mathbf{B}_{T89c}$ (Takahashi et al., 2018). For the selected time interval, the match between the observed and model magnetic fields is very good. A high-pass-filtered version of the SJG data is included at the bottom to emphasize oscillations with frequencies higher than 5 mHz.

The vertical dashed lines in Figures 1d–1l mark the onsets of Pi2 waves that are identified by visually inspecting the filtered SJG H component (Figure 1l). Each onset is associated with positive deflections of the AE index and the unfiltered SJG H component (Figure 1k) and is followed by a toroidal (B_ϕ) wave packet at Arase (Figure 1g), with the exception of the last (0248 UT) onset. The abruptness of the onsets of the Pi2 waves means that the waves were impulsively excited by processes such as rapid reconfiguration of the near-Earth magnetotail and braking of bursty bulk flows. Van Allen Probe B also detected corresponding compressional magnetic field oscillations (Figure 1i), although the first two and the last events are weak.

The GOES-13 proton flux data (Figure 1e) indicate a dip ∼6 min after the 0102 UT Pi2 onset, but nothing remarkable occurred after the other Pi2 onsets. The GOES-13 magnetic field data (Figure 1f) show irregular

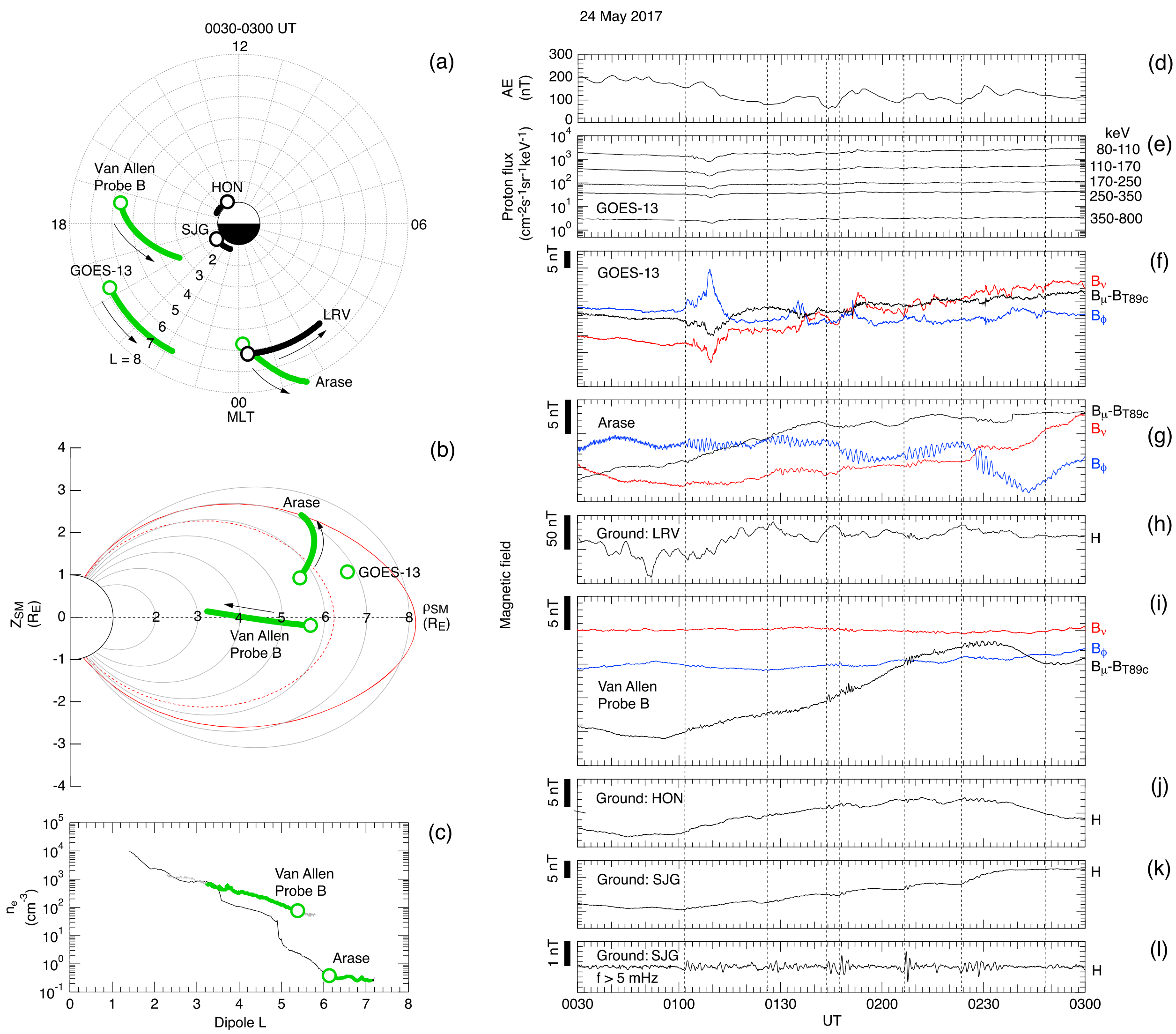

Figure 1. (a) Locations of spacecraft and ground observatories in L-MLT coordinates for the time interval selected for analysis. The open circles indicate the start time 0030 UT. (b) Locations of the spacecraft in SM ρ_{SM}-z_{SM} coordinates, where ρ_{SM} is distance from the dipole axis and z_{SM} is distance from the magnetic equator along the dipole axis. The gray lines illustrate the dipole field. The dashed and solid red lines are T89c model field lines passing Arase at 0100 UT and 0300 UT, respectively. (c) Electron density at Arase for 23 May 2140 UT to 24 May 0300 UT and at Van Allen Probe B for 24 May 0000–0330 UT plotted as a function of L. The thick green portion of the data trace indicates measurements made at 0100–0300 UT. (d–l) Time series plots of quantities described in the text. The ground data are the horizontal northward (H) components. The vertical dashed lines mark the onsets of Pi2 waves at SJG. MLT = magnetic local time; SM = solar magnetospheric; GOES = Geostationary Operational Environmental Satellite.

variations, but there are no clear sudden changes associated with the ground Pi2 onsets except at 0102 UT. These features suggest that there were substorm-type disturbances in the magnetotail but the dipolarization fronts associated with them (Ohtani et al., 2006) did not reach $L < 7$. This is not unexpected considering the weakness of substorms as inferred from the low (<300 nT) AE values.

We examined data from other spacecraft located in the magnetosphere for signatures of ultralow frequency waves related to the waves described above. Van Allen Probe A, which was located at $L = 2.5$–5.6 and MLT = 12.6–16.3 hr, detected oscillations in the B_μ component similar to those observed at Van Allen Probe B. GOES-15, which was located at $L = 6.7$ and MLT = 15.7–18.1 hr, detected amplitude-modulated second harmonic poloidal waves. At GOES-15, the timing of the amplitude modulation was not synchronized with the Pi2 onsets, which is not unexpected because the waves were most likely excited by an instability associated with ring current ions (Southwood, 1976).

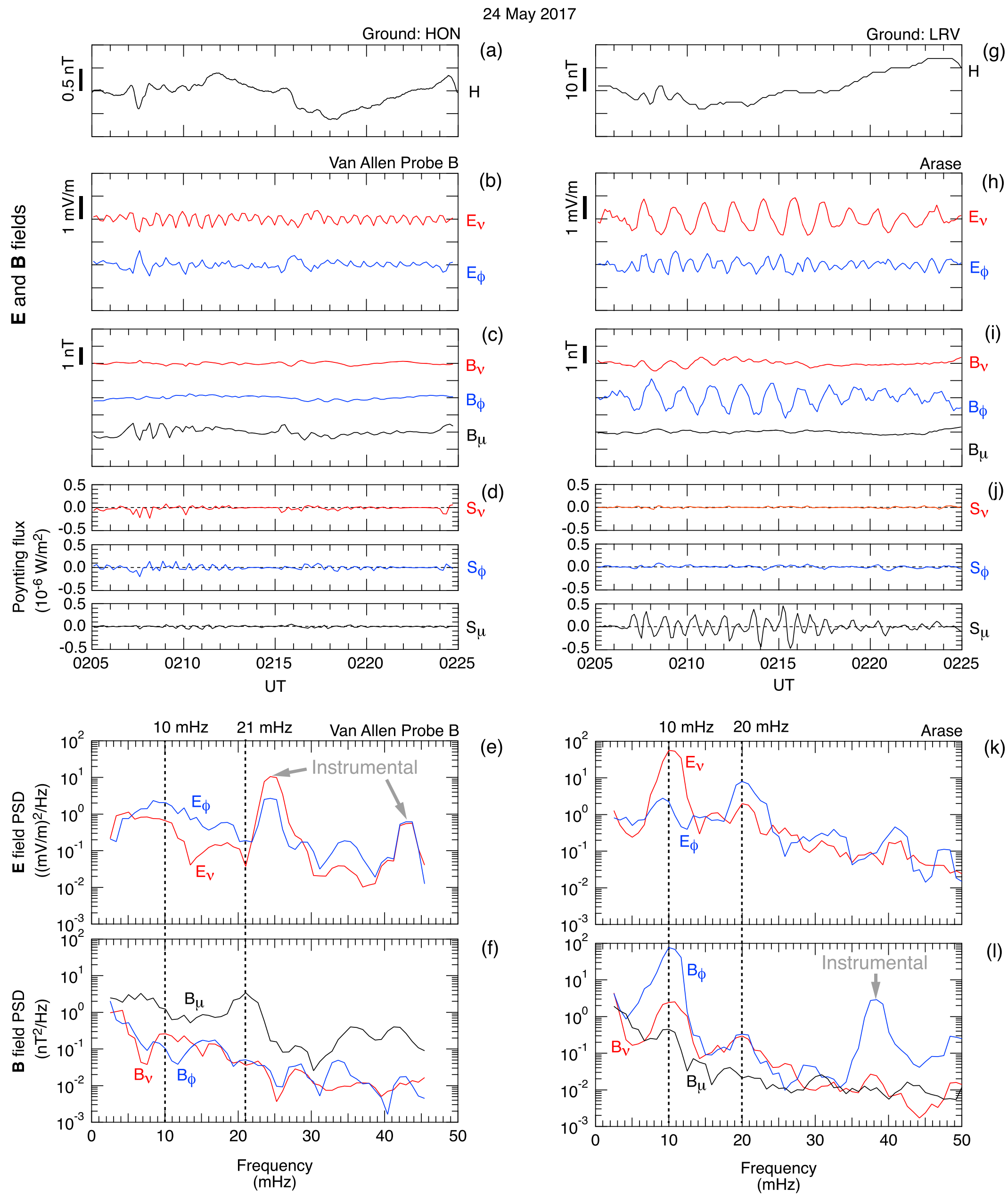

Figure 2. (a) H component at HON. (b, c) Field components at Van Allen Probe B. Each component is detrended by removing a quadratic function fitted to the original data. The high-frequency oscillations seen in the electric field data are an instrumental artifact. (d) Poynting flux. (e, f) Power spectral density computed from the time series data. (g–l) Same as (a)–(f) except for data from LRV and Arase.

Figure 2 compares observations by Van Allen Probe B, Arase, and ground magnetometers during the wave event that started at ~0207 UT. Ground data from HON (Figure 2a) and LRV (Figure 2g) show damped oscillations lasting three to five periods. These oscillations are similar to the compressional magnetic field (B_μ) oscillation detected at Van Allen Probe B (Figure 2c), which produces a spectral peak at 21 mHz (Figure 2f). There is a minor impulse at HON at 0215 UT, which is also associated with a damped B_μ oscillation at Van Allen Probe B. The electric field data from Van Allen Probe B (Figure 2b; Wygant et al., 2013) are contaminated by 25-mHz spacecraft noise, but the broad E_ϕ spectral peak at 10 mHz (Figure 2e) appears to be real. This dual-frequency oscillation at Van Allen Probe B can be explained by simultaneous excitation of the fundamental and second harmonic cavity mode resonances (Luo et al., 2011). Interestingly, the higher-frequency

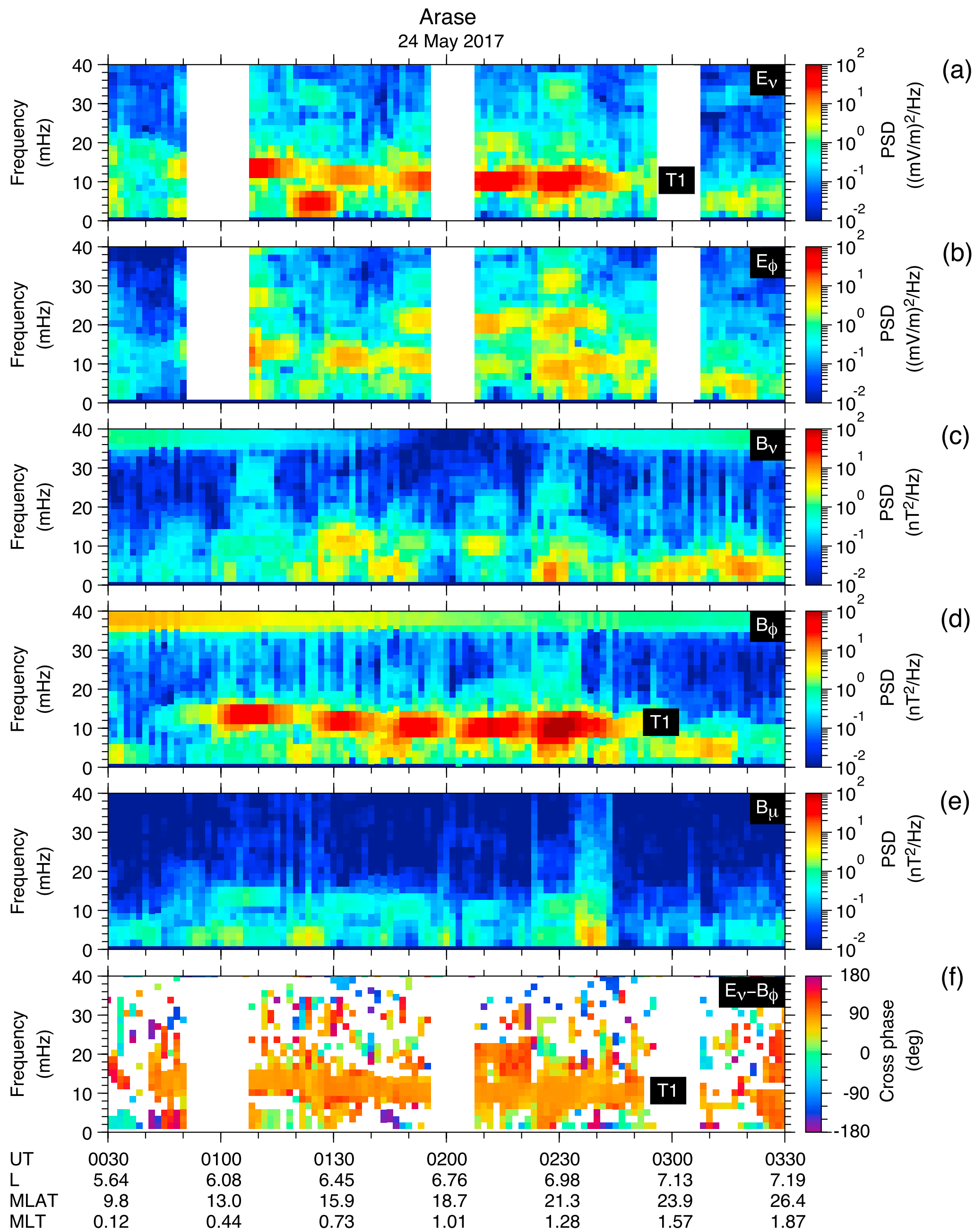

Figure 3. (a–e) Dynamic spectra of the electric and magnetic field data from Arase. The label *T1* indicates the strong oscillation identified to be the fundamental toroidal wave. (f) Cross phase between E_ν and B_ϕ, displayed when the coherence between these components is >0.5. MLAT = magnetic latitude; MLT = magnetic local time.

component was not excited during the event that started at 0224 UT (see Figure 1i). The components of the Poynting flux (Figure 2d) show net earthward energy flow ($S_\nu < 0$) at ~0207 UT, which suggests that an earthward propagating fast mode pulse triggered a Pi2 wave.

Observations at Arase are quite different. At this spacecraft, oscillations appear in the toroidal components, E_ν (Kasaba et al., 2017; Figure 2h) and B_ϕ (Figure 2i), with regular waveforms and spectral peaks at 10 mHz (Figures 2k and 2l). Unlike the quickly damped oscillations seen at Van Allen Probe B and on the ground, the toroidal oscillations lasted ~20 min. Toroidal oscillations with similar properties were detected at Arase following the other Pi2 onsets marked in Figure 1l. The Poynting flux (Figure 2j) shows large oscillations in the S_μ component, with its time average close to zero as expected for standing Alfvén waves.

The E_ν and B_ϕ waveforms are slightly deformed from a pure sinusoid and result in secondary spectral peaks at 20 mHz. This waveform distortion is obviously related to the 20-mHz oscillation that dominates the E_ϕ time series and spectrum. A 20-mHz peak is also found in the B_ν spectrum. We have not identified the cause of the waveform distortion.

Figure 3 shows the persistence of toroidal oscillations at Arase. The dynamic power spectra of the toroidal components (E_ν and B_ϕ) exhibit narrowband enhancement from ~0100 to ~0300 UT (Figures 3a and 3d), with the frequency slowly decreasing from 13 to 10 mHz, consistent with the outward motion of the spacecraft. The amplitude of the waves is modulated, but their frequency is continuous, analogous to fundamental toroidal (T1) waves observed on the dayside (Junginger et al., 1984). Without the knowledge of Pi2 waves that are simultaneously present, one might consider that the toroidal waves are excited by fast mode waves propagating from the dayside (Takahashi et al., 2016). The standing wave nature of the toroidal oscillations is evident from the cross phase (Figure 3f). In the band occupied by the toroidal waves, the phase stays close to +90° (E_ν leads B_ϕ) that is expected for T1 waves observed in the Northern Hemisphere.

Unlike in observations made on the dayside near the magnetic equator (e.g., Engebretson et al., 1986), higher harmonics of the toroidal waves are hardly visible in the E_ν and B_ϕ components when we examine dynamic spectra extended to the Nyquist frequency 63 mHz of the spin-averaged (8-s) time series data. This could mean that the source mechanism excites the fundamental mode preferentially and/or only the fundamental mode appears strongly at the spacecraft location even though higher harmonics were excited.

Concerning the first scenario, a possible explanation is that the disturbances coming from the magnetotail have a MLAT dependence similar to the field line eigenmode structure of the T1 wave, with a peak (antinode) at the magnetic equator. Dayside sources such as interplanetary shocks and foreshock disturbances may have a structure that is more extended in MLAT, which leads to excitation of multiple harmonics.

Concerning the second scenario, we note that theoretical models (e.g., Cummings et al., 1969) indicate that the E_ν amplitude of T1 waves varies little in the MLAT range 13–24° covered by Arase. Meanwhile, the B_ϕ amplitude monotonically increases with MLAT from the equatorial node, making it easier to detect the B_ϕ perturbation at Arase than at geostationary satellites (|MLAT| < 11°). The toroidal waves are similar to those observed by Polar (Keiling et al., 2003). However, Arase differs from Polar in that the former crosses L shells much more slowly at $L \sim 7$.

2.2. Magnetoseismology

Continuous presence of toroidal waves at Arase allows us to estimate the plasma mass density using the magnetoseismic technique developed for other spacecraft (e.g., Takahashi et al., 2004). In this technique, we use the wave equation by Singer et al. (1981) to find the relation between the frequency of the fundamental toroidal wave (denoted f_{T1}) and the mass density ρ. Approximately, we have $f_{T1} \sim [\oint(ds(\mu_0\rho)^{1/2}/B)]^{-1}$, where the integral is taken along the magnetic field line of interest and μ_0 is the permeability of free space. The exact relationship is obtained by numerically solving the wave equation using a model background magnetic field and assuming a functional form of mass density variation along the magnetic field. In this study, we adopt the TS05 model (Tsyganenko & Sitnov, 2005) and assume ρ to vary along the magnetic field lines as $\rho = \rho_0(R_{max}/R)^\alpha$ (e.g., Cummings et al., 1969), where R_{max} is the maximum geocentric distance to a field line, ρ_0 is the mass density at that point, and R is the geocentric distance to any point on the field line. In the present study, we used a slightly modified version of the α model derived by Denton et al. (2014), which gives α values in the narrow range 2.6–3.2 along the Arase orbit between 0030 and 0300 UT.

Figure 4 shows the results of the magnetoseismic analysis. Figure 4a shows the frequencies at the most prominent peaks in the Fourier spectra of the E_ν and B_ϕ components calculated in a 15-min moving data window. These frequencies correspond to the spectral lines labeled T1 in Figure 3. The mass density derived from f_{T1} for the satellite position is shown in Figure 4b along with the electron density n_e. In this figure, the ρ data points lie well above the n_e data points, which means that a substantial number of heavy ions were present and accounted for the bulk of the mass density. Figure 4c shows that the average ion mass M_i $(=\rho/n_e)$ lies in the range 4–8 amu with an average of ~ 6 amu. To account for the average M_i, the O^+ density needs to be between 17% (He-O plasma) and 33% (H-O plasma). According to a statistical analysis of ion composition that is resolved during plasma flow events detected by Time History of Events and Macroscale Interactions during Substorms (Lee & Angelopoulos, 2014), the O^+ number density is higher than the H^+ number density near midnight in the L range 5–12. The lower relative O^+ density that we obtained can be attributed to the

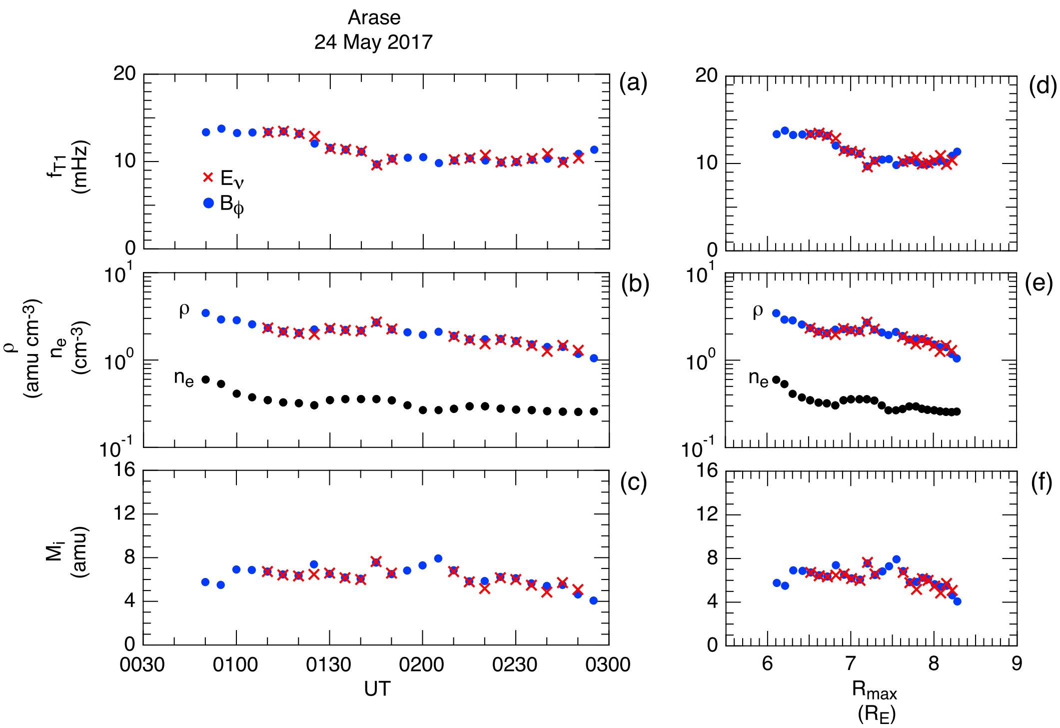

Figure 4. Magnetoseismic analysis of Arase data. (a) Frequency of the fundamental toroidal wave (f_{T1}) determined using the E_v and B_ϕ components. (b) Mass density (red crosses and blue dots) at the spacecraft estimated using f_{T1} and electron density at the spacecraft estimated using plasma wave spectra. (c) Average ion mass (=ρ/n_e). (d–f) Same quantities plotted as a function of distance to the model field line at the farthest point from the center of the Earth.

solar activity dependence of the O^+ density. According to Denton et al. (2011), the O^+ density more strongly depends on the solar activity level (represented by the solar irradiance *F*10.7 index) than the H^+ density. Our measurement was made in 2017 when the solar activity was approaching a minimum, whereas the statistics provided by Lee and Angelopoulos (2014) included measurements made from 2008 to 2013 during which a wide range of solar activity levels occurred.

Previous spacecraft-based magnetoseismic studies most often used equatorial magnetic field observations and reported very low rate (<1%) of detection of toroidal waves at midnight (e.g., Takahashi et al., 2010). Arase, with its higher inclination, is capable of detecting T1 waves in both E_v and B_ϕ more easily than equatorial satellites, which remain near the equatorial B_ϕ node of T1 waves. This makes Arase a valuable resource for magnetoseismic studies, even when the spacecraft is in the midnight sector.

3. Discussion

There are striking differences among the field variations observed by GOES-13, Arase, and Van Allen Probe B. GOES-13 did not detect any magnetic field perturbations or particle flux variations unambiguously associated with the Pi2 onsets detected on the ground and at Van Allen Probe B. This implies that the source disturbances of the Pi2 waves occurred away from GOES-13. The Pi2 source region could have been located at a larger geocentric distance or in the postmidnight sector. The latter is more likely the case because Van Allen Probe B was located on the duskside but detected Pi2 waves.

The duration of the off-equatorial toroidal waves at Arase is much longer than that of the equatorial fast mode waves at Van Allen Probe B. A possible explanation for this observation is that the fast mode is confined in the equatorial region (Lee, 1996) and its coupling to toroidal waves occurs there. Moving away from the equator, the coupled waves quickly lose the fast mode component and exhibit nearly purely transverse magnetic field perturbations. The longer duration of the toroidal waves can be explained by high reflection of Alfvén waves at the ionosphere. According to a model calculation (Takahashi et al., 1996), the nightside ionosphere at $L > 5$ (outside the plasmasphere) has high Pedersen conductivity to sustain long-lasting toroidal waves. Weak ionospheric damping is inferred from the ~90° phase difference between E_v and B_ϕ (Figure 3f) and small (time-averaged) Poynting flux along the magnetic field (Figure 2j). The same calculation showed that the mass density controls the wave period (the real part of frequency) but not the damping rate (the imaginary part of frequency). Therefore, the long life time of toroidal waves outside the plasmasphere appears to be a conductivity effect. It is interesting that the waveform and overall duration of Pi2 waves at Van Allen Probe B and on the ground vary from event to event but the duration and amplitude envelope structure of the T1 waves are remarkably similar.

The T1 waves observed by Arase are not detected by the LRV magnetometer located near the magnetic field footprint of the spacecraft (Figures 2g–2i). This implies that the horizontal scale size of the T1 waves at the ionosphere level is smaller than the effective height (~100 km) of the ionosphere (Glassmeier & Stellmacher, 2000). Here the relevant scale size can be given either in the longitudinal or latitudinal direction. The fact that the fast mode Pi2 waves, which are the likely driver of the toroidal waves, propagated over a long distance to various locations on the ground suggests that the fast mode waves had a long wavelength across the background magnetic field. Therefore, it is likely that the T1 waves initially had a large-scale size as well. As time progresses, however, field lines started oscillating at *L*-dependent frequencies (Anderson et al., 1989). This process produces latitudinally structured ionospheric currents, leading to strong attenuation of T1 wave signals below the ionosphere. In this regard, the current system associated with the present T1 waves differs from large-scale oscillating currents on wedge-shaped circuits that have been proposed to explain globally coherent Pi2 pulsations (Lester et al., 1983; Nishimura et al., 2012).

4. Summary

Impulsively excited nightside toroidal waves have been reported previously (Keiling et al., 2003; Nosé et al., 1998; Takahashi et al., 1996). Using simultaneous electric and magnetic field observations both on and off the magnetic equator obtained with the similarly instrumented Van Allen Probes and Arase spacecraft, we are able to demonstrate the relationship between fast mode and Alfvén mode waves detected at different latitudes. Both wave modes are excited simultaneously, but their duration and ground signatures are vastly different, with significant implication to the wave scale size and ionospheric effects (damping and screening). The long duration of the toroidal waves makes them valuable in magnetoseismic analysis of the mass density.

Acknowledgments
K. T. was supported by NASA Grants NNX15AI95G and NNX17AD34G. R. E. D. was supported by NSF Grant AGS-1105790. This study was supported by The Japan Society for the Promotion of Science, Grant-in-Aid for Scientific Research on Innovative Areas (Grant 15H05815) and Grant-in-Aid for Scientific Research (Grant 16H04056). Part of this study was carried out under the joint research program of the Institute for Space-Earth Environmental Research (ISEE), Nagoya University. The Arase data were provided by the ERG Science Center operated by the Institute of Space and Astronautical Science, Japan Aerospace and Exploration Agency and ISEE/Nagoya University (https://ergsc.isee.nagoya-u.ac.jp/). The ERG data processors are as follows: MGF L2 v01.00 for the magnetic field, PWE/EFD L2 ver01 (3 March 2018) for the electric field, and PWE/HFA L3 ver00.02 for the electron density. The Arase satellite data will be publicly available via ERG Science Center on a project-agreed schedule. Other data are available from the following sources: Van Allen Probes Science Operations Centers located at University of Iowa (http://emfisis.physics.uiowa.edu) and University of Minnesota (http://www.space.umn.edu/missions/rbspefw-home-university-of-minnesota), for Van Allen Probes; NOAA National Centers for Environmental Information (http://satdat.ngdc.noaa.gov), for GOES; Leirvogur Magnetic Observatory (http://cygnus.raunvis.hi.is//halo/lrv.htmland), for the LRV magnetometer; USGS (https://geomag.usgs.gov/ws/edge/), for the HON and SJG magnetometers; and World Data Center for Geomagnetism, Kyoto (http://wdc.kugi.kyoto-u.ac.jp), for the AE and AL indices. W. Kurth is acknowledged for deriving electron density from the spectra of plasma waves detected by Van Allen Probes.

References

Anderson, B. J., Engebretson, M. J., & Zanetti, L. J. (1989). Distortion effects in spacecraft observations of MHD toroidal standing waves: Theory and observations. *Journal of Geophysical Research*, *94*(A10), 13,425–13,445. https://doi.org/10.1029/JA094iA10p13425

Cummings, W. D., O'Sullivan, R. J., & Coleman, P. J. (1969). Standing Alfvén waves in the magnetosphere. *Journal of Geophysical Research*, *74*(3), 778–793. https://doi.org/10.1029/JA074i003p00778

Denton, R. E., Takahashi, K., Thomsen, M. F., Borovsky, J. E., Singer, H. J., Wang, Y., et al. (2014). Evolution of mass density and o^+ concentration at geostationary orbit during storm and quiet events. *Journal of Geophysical Research: Space Physics*, *119*, 6417–6431. https://doi.org/10.1002/2014ja019888

Denton, R. E., Thomsen, M. F., Takahashi, K., Anderson, R. R., & Singer, H. J. (2011). Solar cycle dependence of bulk ion composition at geosynchronous orbit. *Journal of Geophysical Research*, *116*, A03212. https://doi.org/10.1029/2010ja016027

Engebretson, M. J., Zanetti, L. J., Potemra, T. A., & Acuna, M. H. (1986). Harmonically structured ULF pulsations observed by the AMPTE/CCE magnetic-field experiment. *Geophysical Research Letters*, *13*(9), 905–908. https://doi.org/10.1029/GL013i009p00905

Glassmeier, K.-H., & Stellmacher, M. (2000). Concerning the local time asymmetry of Pc5 wave power at the ground and field line resonance widths. *Journal of Geophysical Research*, *105*(A8), 18,847–18,855. https://doi.org/10.1029/2000ja900037

Junginger, H., Geiger, G., Haerendel, G., Melzner, F., Amata, E., & Higel, B. (1984). A statistical study of dayside magnetospheric electric-field fluctuations with periods between 150 and 600 s. *Journal of Geophysical Research*, *89*(7), 5495–5505. https://doi.org/10.1029/JA089iA07p05495

Kasaba, Y., Ishisaka, K., Kasahara, Y., Imachi, T., Yagitani, S., Kojima, H., et al. (2017). Wire Probe Antenna (WPT) and Electric Field Detector (EFD) of Plasma Wave Experiment (PWE) aboard the Arase satellite: Specifications and initial evaluation results. *Earth, Planets and Space*, *69*, 174. https://doi.org/10.1186/s40623-017-0760-x

Kasahara, Y., Kasaba, Y., Kojima, H., Yagitani, S., Ishisaka, K., Kumamoto, A., et al. (2018). The Plasma Wave Experiment (PWE) on board the Arase (ERG) satellite. *Earth, Planets and Space*, *70*, 28. https://doi.org/10.1186/s40623-018-0842-4

Keiling, A., Kim, K. H., Wygant, J. R., Cattell, C., Russell, C. T., & Kletzing, C. A. (2003). Electrodynamics of a substorm-related field line resonance observed by the Polar satellite in comparison with ground Pi2 pulsations. *Journal of Geophysical Research*, *108*(A7), 1275. https://doi.org/1210.1029/2002JA009340

Kletzing, C. A., Kurth, W. S., Acuna, M., MacDowall, R. J., Torbert, R. B., Averkamp, T., et al. (2013). The Electric and Magnetic Field Instrument Suite and Integrated Science (EMFISIS) on RBSP. *Space Science Reviews*, *179*, 127–181. https://doi.org/010.1007/s11214-013-9993-6

Kumamoto, A., Tsuchiya, F., Kasahara, Y., Kasaba, Y., Kojima, H., Yagitani, S., & Obara, T. (2018). High Frequency Analyzer (HFA) of Plasma Wave Experiment (PWE) onboard the Arase spacecraft. *Earth, Planets and Space*, *70*, 82. https://doi.org/10.1186/s40623-018-0854-0

Kurth, W. S., De Pascuale, S., Faden, J. B., Kletzing, C. A., Hospodarsky, G. B., Thaller, S., & Wygant, J. R. (2015). Electron densities inferred from plasma wave spectra obtained by the waves instrument on Van Allen Probes. *Journal of Geophysical Research: Space Physics*, *120*, 904–914. https://doi.org/10.1002/2014JA020857

Lee, D. H. (1996). Dynamics of MHD wave propagation in the low-latitude magnetosphere. *Journal of Geophysical Research*, *101*(A7), 15,371–15,386. https://doi.org/10.1029/96ja00608

Lee, J. H., & Angelopoulos, V. (2014). On the presence and properties of cold ions near Earth's equatorial magnetosphere. *Journal of Geophysical Research: Space Physics*, *119*, 1749–1770. https://doi.org/10.1002/2013ja019305

Lester, M., Hughes, J. W., & Singer, H. J. (1983). Polarization patterns of Pi2 magnetic pulsations and the substorm current wedge. *Journal of Geophysical Research*, *88*(A10), 7958–7966. https://doi.org/10.1029/JA088iA10p07958

Lopez, R. E., Sibeck, D. G., McEntire, R. W., & Krimigis, S. M. (1990). The energetic ion substorm injection boundary. *Journal of Geophysical Research*, *95*, 109–117. https://doi.org/10.1029/JA095iA01p00109

Luo, H., Chen, G. X., Du, A. M., Angelopoulos, V., Xu, W. Y., Zhao, X. D., & Wang, Y. (2011). THEMIS multipoint observations of Pi2 pulsations inside and outside the plasmasphere. *Journal of Geophysical Research*, *116*, A12206. https://doi.org/10.1029/2011ja016746

Matsuoka, A., Teramoto, M., Nomura, R., Nosé, M., Fujimoto, A., Tanaka, Y., & Shinohara, I. (2018). The ARASE (ERG) magnetic field investigation. *Earth, Planets and Space*, *70*, 43. https://doi.org/10.1186/s40623-018-0800-1

Miyoshi, Y., Shinohara, I., Takashima, T., Asamura, K., Higashio, N., Mitani, T., et al. (2018). Geospace exploration project ERG. *Earth, Planets and Space*, *70*, 101. https://doi.org/10.1186/s40623-018-0862-0

Nishimura, Y., Lyons, L. R., Kikuchi, T., Angelopoulos, V., Donovan, E., Mende, S., et al. (2012). Formation of substorm Pi2: A coherent response to auroral streamers and currents. *Journal of Geophysical Research*, *117*, A09218. https://doi.org/10.1029/2012ja017889

Nosé, M., Iyemori, T., Nakabe, S., Nagai, T., Matsumoto, H., & Goka, T. (1998). ULF pulsations observed by the ETS-VI satellite: Substorm associated azimuthal Pc 4 pulsations on the nightside. *Earth, Planets and Space*, *50*(1), 63–80. https://doi.org/10.1186/bf03352087

Ohtani, S., Singer, H. J., & Mukai, T. (2006). Effects of the fast plasma sheet flow on the geosynchronous magnetic configuration: Geotail and GOES coordinated study. *Journal of Geophysical Research*, *111*, A01204. https://doi.org/10.1029/2005ja011383

Osaki, H., Takahashi, K., Fukunishi, H., Nagatsuma, T., Oya, H., Matsuoka, A., & Milling, D. K. (1998). Pi2 pulsations observed from the Akebono satellite in the plasmasphere. *Journal of Geophysical Research*, *103*(A8), 17,605–17,615. https://doi.org/10.1029/97ja03012

Panov, E. V., Baumjohann, W., Nakamura, R., Kubyshkina, M. V., Glassmeier, K. H., Angelopoulos, V., et al. (2014). Period and damping factor of Pi2 pulsations during oscillatory flow braking in the magnetotail. *Journal of Geophysical Research: Space Physics*, *119*, 4512–4520. https://doi.org/10.1002/2013ja019633

Rodriguez, J. V. (2014). *GOES 13–15 MAGE/PD Pitch Angles Algorithm Theoretical Basis Document, Version 1.0* (pp. 28). Silver Spring, MD: NOAA National Geophysical Data Center. Retrieved from http://www.ngdc.noaa.gov/stp/satellite/goes/documentation.html

Samson, J. C., Cogger, L. L., & Pao, Q. (1996). Observations of field line resonances, auroral arcs, and auroral vortex structures. *Journal of Geophysical Research*, *101*(A8), 17,373–17,383. https://doi.org/10.1029/96ja01086

Singer, H. J., Matheson, L., Grubb, R., Newman, A., & Bouwer, S. D. (1996). Monitoring space weather with the GOES magnetometers. *Proceedings of the International Society for Optics and Photonics (SPIE)*, *2812*, 299–308. https://doi.org/10.1117/12.254077

Singer, H. J., Southwood, D. J., Walker, R. J., & Kivelson, M. G. (1981). Alfven wave resonances in a realistic magnetospheric magnetic field geometry. *Journal of Geophysical Research*, *86*(A6), 4589–4596. https://doi.org/10.1029/JA086iA06p04589

Southwood, D. J. (1976). A general approach to low-frequency instability in the ring current plasma. *Journal of Geophysical Research*, *81*(19), 3340–3348. https://doi.org/10.1029/JA081i019p03340

Takahashi, K., Anderson, B. J., & Ohtani, S. (1996). Multisatellite study of nightside transient toroidal waves. *Journal of Geophysical Research*, *101*(A11), 24,815–24,825. https://doi.org/10.1029/96ja02045

Takahashi, K., Denton, R. E., Anderson, R. R., & Hughes, W. J. (2004). Frequencies of standing Alfvén wave harmonics and their implication for plasma mass distribution along geomagnetic field lines: Statistical analysis of CRRES data. *Journal of Geophysical Research*, *109*, A08202. https://doi.org/10.1029/2003ja010345

Takahashi, K., Denton, R. E., & Singer, H. J. (2010). Solar cycle variation of geosynchronous plasma mass density derived from the frequency of standing Alfvén waves. *Journal of Geophysical Research*, *115*, A07207. https://doi.org/10.1029/2009ja015243

Takahashi, K., Hartinger, M. D., Malaspina, D. M., Smith, C. W., Koga, K., Singer, H. J., et al. (2016). Propagation of ULF waves from the upstream region to the midnight sector of the inner magnetosphere. *Journal of Geophysical Research: Space Physics*, *121*, 8428–8447. https://doi.org/10.1002/2016ja022958

Takahashi, K., Lee, D. H., Nosé, M., Anderson, R. R., & Hughes, W. J. (2003). CRRES electric field study of the radial mode structure of Pi2 pulsations. *Journal of Geophysical Research*, *108*(A5), 1210. https://doi.org/10.1029/2002ja009761

Takahashi, K., Lysak, R., Vellante, M., Kletzing, C. A., Hartinger, M. D., & Smith, C. W. (2018). Observation and numerical simulation of cavity mode oscillations excited by an interplanetary shock. *Journal of Geophysical Research: Space Physics*, *123*, 1969–1988. https://doi.org/10.1002/2017ja024639

Tamao, T. (1965). Transmission and coupling resonance of hydromagnetic disturbances in the non-uniform Earth's magnetosphere. The Science Reports of the Tohoku University, Fifth Series. *Geophysics*, *17*, 43–72.

Teramoto, M., Takahashi, K., Nosé, M., Lee, D. H., & Sutcliffe, P. R. (2011). Pi2 pulsations in the inner magnetosphere simultaneously observed by the Active Magnetospheric Particle Tracer Explorers/Charge Composition Explorer and Dynamics Explorer 1 satellites. *Journal of Geophysical Research*, *116*, A07225. https://doi.org/10.1029/2010ja016199

Tsyganenko, N. A. (1989). A magnetospheric magnetic field model with a warped tail current sheet. *Planetary and Space Science*, *37*(1), 5–20. https://doi.org/10.1016/0032-0633(89)90066-4

Tsyganenko, N. A., & Sitnov, M. I. (2005). Modeling the dynamics of the inner magnetosphere during strong geomagnetic storms. *Journal of Geophysical Research*, *110*, A03208. https://doi.org/10.1029/2004ja010798

Wygant, J. R., Bonnell, J. W., Goetz, K., Ergun, R. E., Mozer, F. S., Bale, S. D., et al. (2013). The Electric Field and Waves Instruments on the Radiation Belt Storm Probes mission. *Space Science Reviews*, *179*(1–4), 183–220. https://doi.org/10.1007/s11214-013-0013-7